

High Temperature Oxidation of Spark Plasma Sintered and Thermally Sprayed FeAl-Based Iron Aluminides

P. HAUSILD^{a,*}, M. KARLÍK^a, T. SKIBA^b, P. SAJDL^c, J. DUBSKÝ^d AND M. PALM^e

^aCzech Technical University in Prague, Faculty of Nuclear Sciences and Physical Engineering
Department of Materials, Trojanova 13, 120 00 Prague 2, Czech Republic

^bResearch Centre Rez Ltd., Husinec-Rez 130, 250 68 Rez, Czech Republic

^cInstitute of Chemical Technology Prague, Technická 5, 166 28 Prague 6, Czech Republic

^dInstitute of Plasma Physics AS CR, v. v. i., Department of Materials Engineering
Za Slovankou 3, 182 00 Prague 8, Czech Republic

^eMax-Planck-Institut für Eisenforschung GmbH, Max-Planck-Str. 1, D-40237 Düsseldorf, Germany

The presented work deals with the oxidation resistance of spark plasma sintered and thermally sprayed FeAl-based intermetallics. Gas-atomized binary single phase Fe-43(at.%)Al and dual phase Fe-55(at.%)Al powders were used for spark plasma sintering and/or thermal spraying. Coatings were deposited by two different plasma spray technologies — gas and water stabilized plasma guns. The prepared samples were exposed to oxidation in artificial air at 700 °C. The mass gain was measured during oxidation at 700 °C up to 1000 h. Microstructures, phase and chemical compositions of the formed scales were characterized after the exposition by means of scanning electron microscopy, X-ray diffraction and electron spectroscopy for chemical analysis (X-ray photoelectron spectroscopy).

PACS: 81.05.Bx, 81.65.Mq, 81.20.Ev, 81.15.Rs

1. Introduction

The excellent high temperature oxidation resistance of Al-rich iron aluminides is due to the formation of alumina scales [1–3], which form readily above approximately 500 °C [4]. The best oxidation protection is obtained by α -Al₂O₃, which is stable in binary Fe–Al above 900 °C [5, 6]. At lower temperatures, less effective but still protective Al₂O₃ polytypes form, e.g. θ - or γ -Al₂O₃ [7].

The major weakness of FeAl based intermetallic alloys is their brittleness at room temperature [8–11]. Because of the difficulties in conventional metallurgical processing of iron aluminides with Al contents higher than 40 at.% research efforts have focused on powder metallurgy [12–16] or thermal spray techniques [17–23]. Among the powder metallurgical techniques, spark plasma sintering (SPS) offers very fast densification which is important to maintain the initial grain (powder) size in the sintered material.

Among the thermal spray techniques, high velocity oxy-fuel (HVOF) spraying is the most used to produce thick coatings from FeAl powders. However, gas stabilized plasma (GSP) or water stabilized plasma (WSP)

torches can provide much higher feed-rates than HVOF and are therefore more suitable for depositing protective layers on larger surfaces.

Although there has been an extensive research on high temperature oxidation behaviour of FeAl iron aluminides, the majority of published papers deals with bulk samples and/or is limited to temperatures above 800 °C. The purpose of present work is to characterize the oxidation behaviour at 700 °C of SPS and plasma sprayed binary FeAl alloys.

2. Experimental details

The feedstock materials were atomized powders with compositions of Fe-43at.%Al and Fe-56at.%Al. The powders were denoted SP (single phase) and DP (dual phase), as they contain B2 FeAl only and FeAl plus decomposed ε eutectoid (FeAl + FeAl₂), respectively. The powders were sieved into size fractions < 32, 50–90 and 90–140 μ m, which were used for SPS, GSP and WSP, respectively. The spark plasma sintering of compact specimens was carried out in a FCT HP D 25/1 FAST device. FeAl powders were also deposited on low carbon steel substrates by two plasma spraying technologies: gas stabilized plasma torch SulzerMetco F4 and water stabilized plasma torch PAL 160. Due to the lower quantity of the

* corresponding author; e-mail: Petr.Hausild@jfi.cvut.cz

feedstock powder, the DP coatings were obtained only by GSP torch. Further processing details as well as the mechanical properties of FeAl SPS compacts and plasma sprayed coatings can be found in Refs. [24, 25].

SPS compacts and plasma sprayed coatings (removed from the substrate) were cut by a diamond saw into rectangular samples and used for thermogravimetric oxidation tests in a Setaram SETSYS 16/18 thermobalance. Samples were oxidised in synthetic air (20.5% O₂ and 79.5% N₂) at 700 °C up to 1000 h with continuous recording of the mass gain.

Microstructures before and after oxidation tests were studied using scanning electron microscopes (SEM) JEOL JSM 7500 F with cold field emission gun (at acceleration voltage 2 kV) and JEOL JSM-5510 LV (at acceleration voltage 20 kV) equipped with an energy-dispersive X-ray spectrometer (EDS) IXRF500. Phase identification was performed by X-ray diffraction (XRD) using a Siemens D500 diffractometer with Cr K_α and Cu K_α cathodes. Surface chemical analysis was carried out by X-ray photoelectron spectroscopy (XPS) on an Omicron Nanotechnology ESCA Probe P. Before XPS analysis, the surface layer of ≈ 30 nm thickness was etched by an ion gun (Ar ions, 5 kV) to avoid adventitious hydrocarbons adsorbed from the atmosphere.

3. Results and discussion

The microstructures of both SPS SP and DP specimens were homogeneous with only very low amounts of fine pores and remnants of fine oxides on particle boundaries [24]. For all the plasma sprayed coatings the typical microstructure consisted of flattened splats created from fully molten powders and partially unmolten particles. Oxides, pores and cracks were present in the coating (Fig. 1). EDS revealed localized depletion of Al. Mean Al depletion was 5 at.% and 4 at.% in the case of SP and DP coatings, respectively.

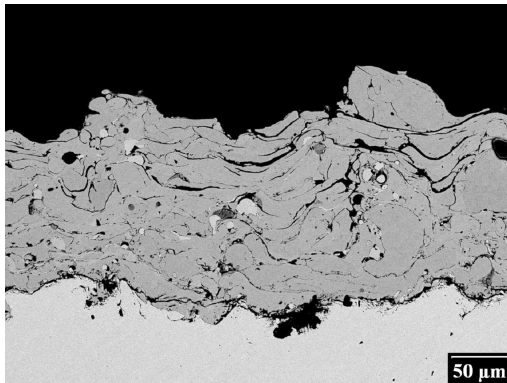


Fig. 1. Microstructure of the plasma sprayed coating (GSP SP).

The kinetics of oxidation measured by thermogravimetry at 700 °C is illustrated in Fig. 2 by showing the specific mass gain vs. time in a parabolic scale. Since diffu-

sion processes in the oxide scale are rate determining for the oxidation, the kinetics can generally be described by the parabolic rate law of diffusion controlled oxidation, even if the measured kinetics in wide temperature ranges do not closely correspond to this law

$$\frac{\Delta m}{S} = \sqrt{k_p t}, \quad (3.1)$$

where Δm is the mass gain, S is the sample surface, k_p is the parabolic rate constant, t is the time.

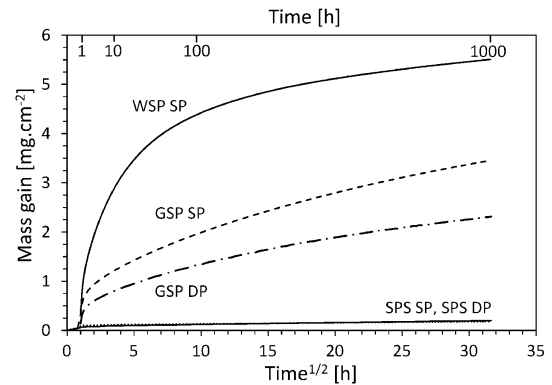


Fig. 2. The kinetics of oxidation measured by thermogravimetry at 700 °C.

All samples show a continuous decrease in the slope of the parabolic plot up to the end of the test. The data clearly indicate different oxidation kinetics for the SPS and plasma sprayed samples. The specific mass gain was considerably higher in the case of plasma sprayed samples and the steady-state parabolic rate constants were two orders of magnitude higher than in the case of SPS samples (Table). No drops due to spallation of the formed scales can be noticed on the measured thermogravimetric curves for any of the investigated samples.

TABLE

Parabolic rate constants (estimated from record between 400 and 1000 h) and the oxide type after the oxidation test (XRD).

Sample	k_p [g ² cm ⁻⁴ s ⁻¹]	Oxide type
SPS SP	3.21×10^{-15}	Al ₂ O ₃
SPS DP	1.23×10^{-15}	Al ₂ O ₃
GSP SP	8.77×10^{-13}	Al ₂ O ₃
GSP DP	3.56×10^{-13}	Al ₂ O ₃
WSP SP	3.04×10^{-13}	Al ₂ O ₃ , Fe ₂ O ₃

FeAl alloys have been extensively studied at temperatures above 800 °C e.g. Refs. [6, 19, 22, 26, 27]. Unfortunately, the occurrence of different polytypes of Al₂O₃ at higher temperatures or in different environments makes it difficult to extrapolate the results obtained at higher temperatures to the experiments performed in this work. The measured values of the parabolic rate constants k_p

of our SPS materials are slightly higher than those obtained for an Fe–25Al–2Ta (at.%) alloy studied under the same conditions (700 °C, 1000 h) [28]. As the present results once more reveal that the oxidation behaviour improves with increasing Al content, i.e. the parabolic rate constants k_p of the DP materials are always lower than those of the SP materials, the considerable smaller grain size of the present materials could be responsible that the parabolic rate constants k_p of these powder metallurgical processed materials are slightly higher than those obtained for the as-cast Fe–25Al–2Ta (at.%) alloy.

After oxidation test, XPS analysis carried out on SPS SP, SPS DP, GSP DP and WSP SP samples revealed the presence of aluminium oxide (all samples) and iron oxide (plasma sprayed). Aluminium oxide was identified as Al_2O_3 -type with Al line $2p_{3/2}$ and binding energy ≈ 74.5 eV. The oxide layer was too thin for XRD in the Bragg–Brentano geometry except the WSP SP sample in which Fe_2O_3 (hematite) was found. In other samples, grazing incidence (at angle of 3°) geometry revealed $\gamma\text{-Al}_2\text{O}_3$ (Fig. 3).

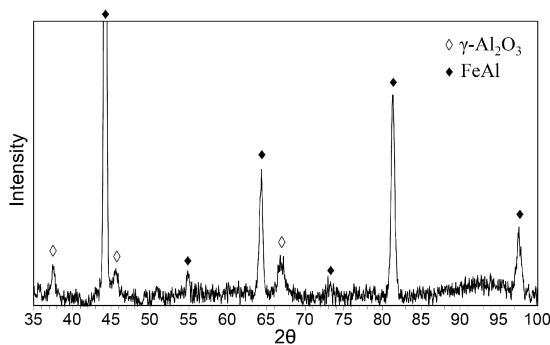


Fig. 3. XRD phase identification after the oxidation test (GSP SP).

SEM observation of oxidized SPS SP and DP samples confirmed a compact oxide scale after the tests (no spallation or cracking of the oxide scale). The morphology of the oxide scale can be seen in Fig. 4. For the plasma sprayed samples (GSP, WSP), a similar morphology of the alumina oxide scale is observed on the splats surface (Fig. 4b) but the particles are coarser compared to the SPS bulk samples surface (Fig. 4a). Besides Al_2O_3 , the Fe_2O_3 oxides in form of nodules were identified by EDS in the plasma sprayed samples. These nodules were covered by whisker-like aluminium oxide fibres growing from underlying Fe_2O_3 (Fig. 4c). The highest density of Fe_2O_3 nodules with whisker-like aluminium oxides was found in the WSP SP sample. Also, the WSP SP coatings exhibited the highest oxidation kinetics in the initial stage and then slightly lower than kinetics observed for GSP SP and GSP DP (for $t > 200$ h). This is most likely due to the fact that even if aluminium has a thermodynamically higher tendency to form Al_2O_3 than iron does have to form Fe_2O_3 , the latter grows faster causing a rapid mass gain. When the protective Al_2O_3 scale is

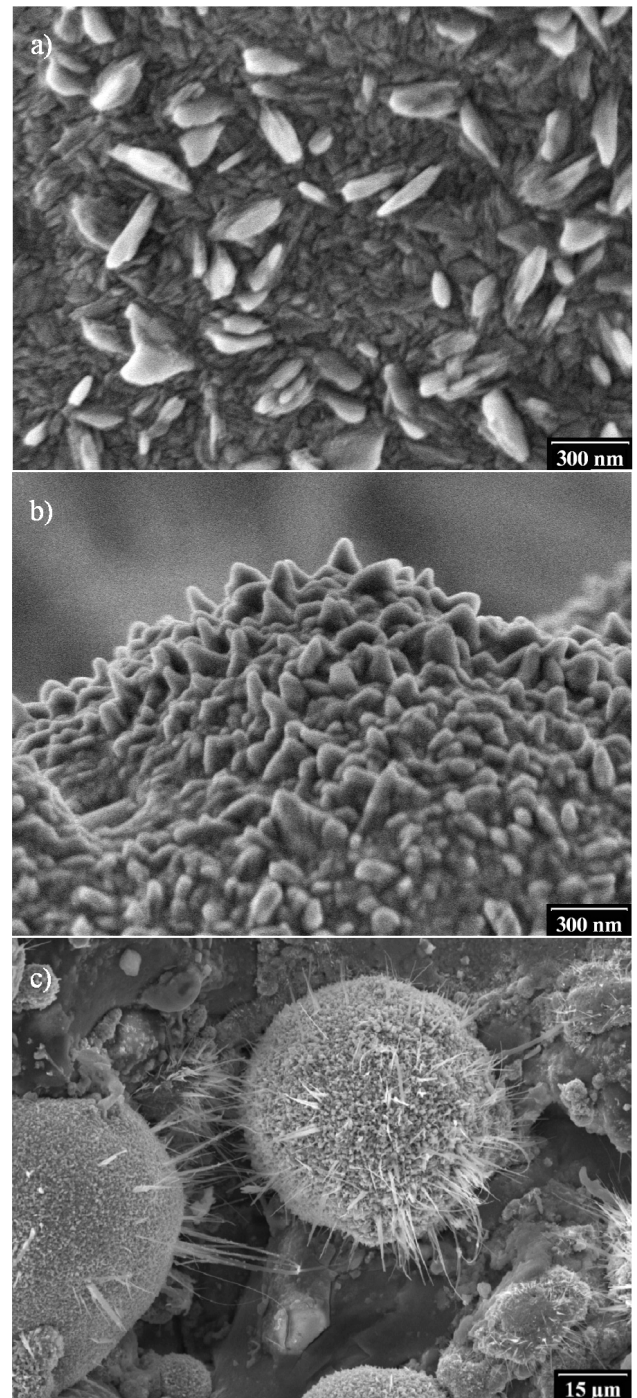


Fig. 4. Oxide scale morphology after 1000 h oxidation at 700 °C: (a) SPS SP, (b) GSP SP, (c) WSP SP.

formed beneath the Fe_2O_3 oxide, the coatings regain a good oxidation resistance as shown by a decrease of k_p .

4. Conclusions

The oxidation behaviour of spark plasma sintered and plasma sprayed binary Fe–43at.%Al and Fe–56at.%Al

powders was characterized in synthetic air at 700 °C. The results can be summarized as follows:

1. The SPS samples formed compact, well-adherent Al₂O₃ scales which show slow oxidation kinetics. No spallation, cracking or cavity formation was observed.
2. The oxidation kinetics of the plasma sprayed samples is significantly faster than that of the SPS samples due to a higher roughness of the plasma sprayed samples and a heterogeneous composition of the coatings.
3. Uneven Al depletion in the plasma sprayed coatings can lead to local changes from protective Al₂O₃ scale to Fe₂O₃ formation if the local Al content is lower than critical for alumina formation. A good control of the spray parameters is therefore an essential step towards oxidation resistant iron aluminide coatings.

Acknowledgments

This research has been supported by the Czech Technical University in Prague SGS grant 10/300/OHK4/3T/14.

References

- [1] W.C. Hagel, *Corrosion* **21**, 316 (1965).
- [2] B. Schmidt, P. Nagpal, I. Baker, in: *High-Temperature Ordered Intermetallic Alloys III, MRS Symp. Proc.*, Vol. 133, Eds. C.T. Liu, A.I. Taub, N.S. Stoloff, C.C. Koch, Materials Research Society, PA 1989, p. 755.
- [3] J.R. Stephens, in: *High-Temperature Intermetallic Ordered Alloys, MRS Symp. Proc.*, Vol. 39, Eds. C.C. Koch, C.T. Liu, N.S. Stoloff, Materials Research Society, PA 1985, p. 381.
- [4] P.F. Tortorelli, K. Natesan, *Mater. Sci. Eng. A* **258**, 115 (1998).
- [5] R. Prescott, M.J. Graham, *Oxid. Met.* **38**, 73 (1992).
- [6] I. Rommerskirchen, B. Eltester, H.-J. Grabke, *Mater. Corros.* **47**, 646 (1996).
- [7] M. Sakiyama, P. Tomaszewicz, G.R. Wallwork, *Oxid. Met.* **13**, 311 (1979).
- [8] J.H. Schneibel, in: *Processing, Properties, and Applications of Iron Aluminides*, Eds. J.H. Schneibel, M.A. Crimp, TMS, Warrendale, PA, 1994, p. 329.
- [9] I. Baker, P.R. Munroe, *Int. Mater. Rev.* **42**, 181 (1997).
- [10] P. Haušild, J. Siegl, P. Málek, V. Šíma, *Intermetallics* **17**, 680 (2009).
- [11] N.S. Stoloff, *Mater. Sci. Eng. A* **258**, 1 (1998).
- [12] D.G. Morris, S. Gunter, *Mater. Sci. Eng. A* **208**, 7 (1996).
- [13] Y. Minamino, Y. Koizumi, N. Tsuji, N. Hirohata, K. Mizuuchi, Y. Ohkanda, *Sci. Technol. Adv. Mater.* **5**, 133 (2004).
- [14] S. Paris, E. Gaffet, F. Bernard, Z.A. Munir, *Scr. Mater.* **50**, 691 (2004).
- [15] G. Ji, T. Grosdidier, N. Bozzolo, S. Launois, *Intermetallics* **15**, 108 (2007).
- [16] L. D'Angelo, L. D'Onofrio, G. Gonzalez, *J. Alloys Comp.* **483**, 154 (2009).
- [17] T. Grosdidier, G. Ji, F. Bernard, E. Gaffet, Z.A. Munir, S. Launois, *Intermetallics* **14**, 1208 (2006).
- [18] J.M. Guilemany, C.R.C Lima, N. Cinca, J.R. Miguel, *Surf. Coat. Technol.* **201**, 2072 (2006).
- [19] J.M. Guilemany, N. Cinca, S. Dosta, C.R.C Lima, *Intermetallics* **15**, 1384 (2007).
- [20] T. Grosdidier, H.L. Liao, A. Tidu, in: *Thermal Spray: Surface Engineering via Applied Research*, Ed. C.C. Berndt, ASM International, Materials Park, OH 2000, p. 1341.
- [21] C. Xiao, W. Chen, *Surf. Coat. Technol.* **201**, 3625 (2006).
- [22] N. Masahashi, S. Watanabe, S. Hanada, *ISIJ Int.* **41**, 1010 (2001).
- [23] J. Xiang, X. Zhu, G. Chen, Z. Duan, Y. Lin, Y. Liu, *Trans. Nonferrous Met. Soc. China* **19**, 1545 (2009).
- [24] T. Skiba, P. Haušild, M. Karlík, K. Vanmeensel, J. Vleugels, *Intermetallics* **18**, 1410 (2010).
- [25] R. Mušálek, O. Kovářík, T. Skiba, P. Haušild, M. Karlík, J. Colmenares-Angulo, *Intermetallics* **18**, 1415 (2010).
- [26] M. Palm, G. Sauthoff, *Intermetallics* **12**, 1345 (2004).
- [27] P. Novák, M. Zelinková, J. Šerák, A. Michalcová, M. Novák, D. Vojtěch, *Intermetallics* **19**, 1306 (2011).
- [28] A. Hotař, M. Palm, *Intermetallics* **18**, 1390 (2010).